



# Co-firing of high-ash discard coal and refuse-derived fuel – ash and gaseous emissions

by K. Isaac<sup>1</sup> and S.O. Bada<sup>1</sup>

## Affiliation:

<sup>1</sup>DSI-NRF SARChI Clean Coal Technology Research Group, School of Chemical & Metallurgy, Faculty of Engineering and the Built Environment, University of the Witwatersrand, South Africa.

## Correspondence to:

S.O. Bada

## Email:

Samson.Bada@wits.ac.za

## Dates:

Received: 9 Feb. 2022

Revised: 31 Mar. 2022

Accepted: 5 Apr. 2022

Published: August 2022

## How to cite:

Isaac, K. and Bada, S.O. 2022  
Co-firing of high-ash discard coal and refuse-derived fuel – ash and gaseous emissions.  
Journal of the Southern African Institute of Mining and Metallurgy, vol. 122, no. 8, pp. 451–460

## DOI ID:

<http://dx.doi.org/10.17159/2411-9717/2015/2022>

## ORCID:

S.O. Bada  
<https://orcid.org/0000-0002-1079-3492>

## K. Isaac

<https://orcid.org/0000-0001-5934-9280>

## Synopsis

This research focuses on the co-firing of discard coal with refuse-derived fuel (RDF) to utilize this abundant resource in South Africa for energy generation and reduce the volume of waste disposed of at landfills. The potential of a coal with a high ash content (> 40%), which is a grade used in some power stations in South Africa, and its combustion compatibility with two different RDFs in terms of emission reductions has been established. Gaseous emissions and ash residues from the combustion and co-combustion of the coal, two different RDFs and coal/RDF blends of different proportion were analysed. One of the RDF samples contained mostly paper (PB) and the other mostly plastic (PL). Co-combustion ash from the discard coal and RDFs showed a decrease in chloride and alkali metal contents as the coal ratio in the blend increased. The slagging propensity of the co-fired blends was found to be very low, while the propensity for fouling decreased from high to medium for all the blends with < 75% RDF. Co-combustion of RDF with coal showed a decrease in SO<sub>2</sub> emissions from 387 ppm (discard coal) to 50 ppm for the sample containing 25% coal discard plus 75% PL. A 15% PL to 85% coal blend also reduced NO<sub>x</sub> emissions from 145 ppm (100% PL) to 88 ppm. The lowest CO<sub>2</sub> emission observed was 6000 ppm for the blend of 85% discard coal plus 15% PB. It was established that the most favourable fuel blend that can produce the lowest sulphur emissions if used for power generation is the 25% coal discard plus 75% PL sample.

## Keywords

ash, co-combustion, discard coal, emissions, refuse-derived fuel.

## Introduction

Coal is the predominant fuel for used electricity and power generation in South Africa. Nearly all the country's carbon reductants in the metallurgical industry, and heat and power for up to 6 000 industrial users such as pulp and paper, cement, sugar, mining, and agriculture, are produced from coal (FFF, 2017). Most of the remaining coal deposits in South Africa are of low quality and need to be beneficiated before they can be used locally or as high-quality marketable products. Locally available low-quality middling is used in Eskom's (South Africa's power utility) pulverized fuel boilers to generate electricity. A power plant like Lethabo uses coal with an average calorific value of 16 MJ/kg and an ash content between 35% and 42% (Eskom, n.d.). The combustion of such coal with a high inherent mineral content leads to air pollution, with emissions of particulate matter, carbon dioxide, sulphur dioxide and oxides of nitrogen (Iacovidou *et al.*, 2018).

The adverse effect of air pollutants from coal-fired power plants on the environment and human health has resulted in many regulations being put in place to reduce the use of fossil fuels for energy generation. These emissions could be reduced by co-firing refuse-derived fuel (RDF) and other types of biomass with coal, because of their lower sulphur content (Vekemans and Chaouki, 2016; Makwarela, Bada, and Falcon, 2017; Malat'ák, Velebil, Bradna, 2018; Ndou *et al.*, 2020). With significant coal deposits in South Africa, coal will continue to play a part in the countries's energy mix over the coming decades. However, coal combustion contributes to CO<sub>2</sub> and SO<sub>x</sub> emissions, and has been deemed harmful to the environment (Cheng and Zhang, 2018). The co-combustion of coal with municipal solid waste (MSW) is one of the promising clean coal technologies that can limit the emissions of greenhouse gases. This is a popular and direct means of reducing the CO<sub>2</sub> intensity of newly designed and existing or older coal-fired power plants.

# Co-firing of high-ash discard coal and refuse-derived fuel – ash and gaseous emissions

Over 2.01 Gt of waste were produced worldwide in 2016, and this is expected to increase to 3.4 Gt by 2050 (World Bank, 2019). Of the 54.2 Mt of waste generated in South Africa per year, only 38.6% is recycled and 61.4% is dumped in landfills (DEA, 2018). In South Africa, land filling used to be the dominant choice for both general and hazardous waste management. However, in 2012 South Africa updated its waste management strategy to minimize landfilling and use the waste rather than collect and dispose of it (DEA, 2012). Given this approach, it is very important to investigate the use of the combustible fraction of this resource for power generation, either alone or co-fired with coal. In this research, the energy potential of different batches of sorted waste streams collected from an environmental waste management establishment in South Africa was investigated. The reactivity of these RDFs and their effect where co-combustion with South African inertinite high-ash coal is discussed.

Several investigations have been carried out on the co-combustion of biomass, sewage sludge, and RDF with the sole purpose of reducing emissions. Akdag, Atimtay, and Sanin 2016 studied the co-combustion of RDF and coal, and reported a decrease in SO<sub>2</sub> emissions as the RDF in the blend increased, with no marked change in NO<sub>x</sub> emission. They also noted a rapid formation of CO that corresponded to a large reduction in oxygen, and attributed this to the high volatile matter content of the RDF. A similar study on SO<sub>2</sub> emissions was carried out by Zhang *et al.* 2018, where a decrease in SO<sub>2</sub> emissions was achieved as the MSW in the coal/MSW blend increased. The authors suggested that this could be due to the adsorption of SO<sub>2</sub> by the pores of the fly ash produced from the coal. In the same study a decrease in NO<sub>x</sub> emissions was noted as the percentage of MSW in the blend increased. This was contrary to the observation made by Akdag, Atimtay, and Sanin 2016 and therefore it is essential that boiler design takes the fuel characteristics into account.

One of the major concerns with RDF combustion is the adverse effect of the fly ash produced on the boiler. The ash from RDF incineration has a high slagging and fouling tendency due to the large proportions of alkaline elements and volatile inorganic oxides such as Na<sub>2</sub>O and K<sub>2</sub>O in the ash (Akdag, Atimtay, and Sanin 2016). The alkali metals in the RDF are released at lower temperatures, and once vaporized can react to form alkali silicates, sulphates, and chlorides (Vekemans and Chaouki, 2016). RDF contains higher chlorine levels than coal. Biomass combustion, depending on type and age, is known to form HCl vapour or chlorides that condense on the walls of the furnace, causing corrosion (Vekemans and Chaouki 2016). The formation of chloride in the furnace reduces the softening temperature of the furnace deposits and damages the protective oxide layer on the furnace surface (Vekemans and Chaouki 2016). It is important that preliminary experimental studies are conducted on the ash produced from the co-combustion of the RDFs utilized in this study with discard coal before recommending RDF as a co-fired fuel. This information is important to the local energy sector, as the majority of the sorted RDFs in the country are exported rather than utilized for power generation. According to Brew (2021) RDF has contributed up to a 50% reduction in MSW landfill in the UK, and the majority of this waste is used in the waste-to-energy facilities.

There is little information on the use of high-ash coal (> 40%) co-fired with RDFs and its impact on the reduction of chlorine and gas emissions. Therefore, in this study, coal with a high ash content, which is of lower quality than the coal used in the

pulverized fuel boilers in the Northern Hemisphere, was tested. Its influence on the elemental composition, i.e., chemistry of the ash produced during co-combustion with different types of RDF (30% plastic blend, 75% plastic blend, 30% paper blend, and 75% paper blend) was studied.

## Materials and methods

### Materials

The discard coal (C2) used in this study was sourced from the Witbank Coalfield in Mpumalanga Province, South Africa. The RDF samples were sourced from Interwaste, an environmental solution, company based in Johannesburg. The waste included cardboard, paper, plastics, and textiles from a range of different product packages. The waste was shredded on site in a primary and secondary shredder to reduce the particle size of the composites. The RDF sample PB (paper blend) contained 53% brown paper and cardboard, 32% yellow coated paper, 10% plastic, and 5% textiles, while the RDF PL (plastic) sample contained 85% plastic, 10% paper, and 5% textiles. The RDF samples were milled in a Retsch SM 200 cutting mill to -212 µm. The discard coal was crushed in a hammer mill and then pulverized to -212 µm. Co-combustion blends of 85% discard coal plus 15% RDF, 70% discard coal plus 30% RDF, 50% discard coal plus 50% RDF, and 25% discard coal plus 75% RDF were used.

### Analytical techniques

#### Gaseous emissions analysis

A diagram of the horizontal tube combustion reactor used for these tests can be seen in Figure 1. The reactor temperature was set to 850°C and 100 mg samples of each blend were combusted in air, at a flow rate of 23 ml/s. The concentration of the gases emitted during combustion was measured with the a Födisch MGA 11 online analyser at a rate of one scan per second over a ten-minute period. Each test was repeated three times and the mean concentrations of each emitted gas used to plot the emission profiles.

#### Ash analyses

The samples were ashed in a furnace in an air atmosphere in accordance with the GEN/TS 14775:2009 standard for 'Solid biofuels - Determination of ash content' and 1171:2010 for 'Solid mineral fuels - Determination of ash'. The ash samples were prepared for SEM/EDX analysis by mounting on stainless steel stubs, and coated with one coat of carbon and two coats of Au/Pd. The samples were then analysed using a Carl Zeiss Sigma FE-SEM. The XRF analysis was conducted using an Ametek SPECTRO XEPOS HE analyser. Approximately 3 g of each sample was used for chloride analysis using a Mertohtm Eco ion chromatography analyser with an aqueous multi-element standard.

The propensity of the fuel to slagging and fouling was predicted using the weight percentage of each compound in the base-to-acid ratio in Equation [1] (James *et al.*, 2012). Where the R<sub>b/a</sub> value is between 0.4 and 0.7, the slagging potential of the ash is considered high or severe, whereas when the value is less than 0.4 or greater than 0.7 the slagging propensity is low to medium (Miller, 2011).

$$R_{b/a} = \frac{Fe_2O_3 + CaO + MgO + K_2O + Na_2O}{SiO_2 + TiO_2 + Al_2O_3} \quad [1]$$

# Co-firing of high-ash discard coal and refuse-derived fuel – ash and gaseous emissions

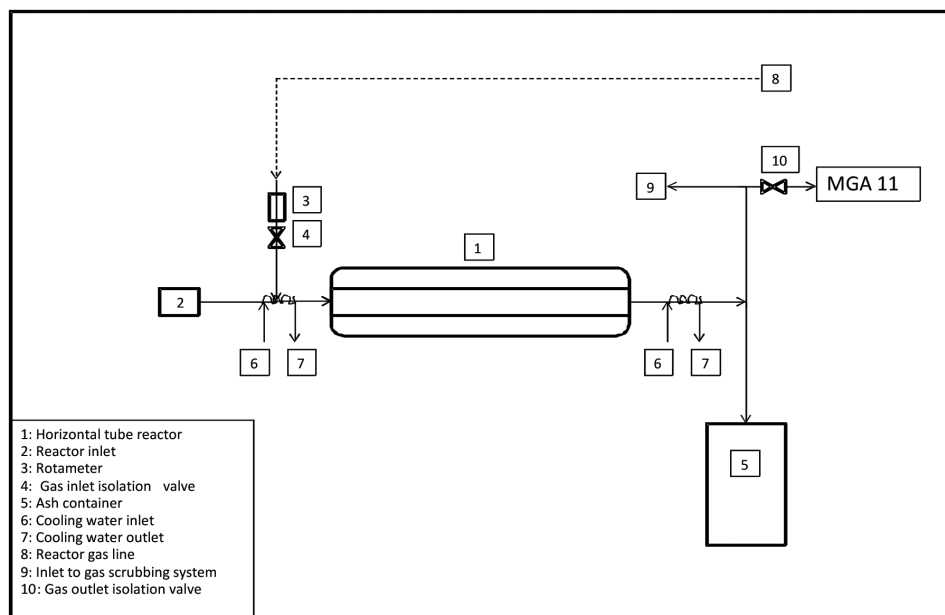


Figure 1—Horizontal tube combustion reactor set-up for gaseous emissions tests

The fouling index is presented in Equation [2]. The fouling potential is low when  $F_u$  is less than 0.6, medium when  $F_u$  is between 0.6 and 1.6, high when  $F_u$  is between 1.6 and 40, and extremely high when the index is above 40 (James *et al.*, 2012).

$$F_u = R_{B/A} \times (Na_2O + K_2O) \quad [2]$$

## Results and discussion

### Physiochemical analysis

Table I presents the physiochemical properties of the discard coal, paper blend, and plastic RDF used in this study. The discard coal possesses the lowest volatile matter content of 20.17%, with the RDFs ranging from 81.15 – 81.67%. With a volatile matter content of 22.88%, the coal is expected to have a higher ignition temperature and lower flame stability than the two RDFs. The three samples had a low moisture content, ranging from 1.23 to 3.19% (inherent moisture). The RDFs had a low fixed carbon (6 – 9%) and ash (6.66%–11.11%) content, while the coal discard had an ash content of 41.95%. The coal discard used in this study can be categorized as a commercial low-grade (grade D III) coal due to its calorific value of 16.73 MJ/kg (Setsepu, Abdulsalam, and Bada, 2021). Furthermore, the fixed carbon content (35.83%) is close to that of coals sampled from three commercial South African coal-fired plants (40.3–46.8%) reported by Rautenbach *et al.* (2019).

The RDF samples had a total carbon content of 57.16% for PB and 57.38% for PL (Table I). The discard coal had a total carbon content of 48.90%, which was expected because it also has the lowest fixed carbon content of all the fuels. The hydrogen content of the RDFs was found to be higher than that of the discard coal, which is in line with the higher volatile matter content of the RDFs. From the same table, it can be seen that the nitrogen content is much lower in the RDF samples (0.29% for PB and 0.35% for PL) compared to the coal sample (1.15%). It is well known that the nitrogen and sulphur content of fuels contributes to the formation of  $NO_x$  and  $SO_x$  during combustion. Therefore, it could be expected that the co-combustion of these RDFs with this coal might lead to a reduction in  $NO_x$  and  $SO_2$  emissions.

### $SO_2$ emissions

The concentrations of  $SO_2$  emitted from the co-combustion of discard coal with plastic (PL) and paper blend (PB) RDF are depicted in Figures 2 and 3, respectively. The discard coal (C2) sample emitted the highest  $SO_2$  concentration, with a peak of 387 ppm at 61 seconds. This shows that the volatile combustion stage was the dominant stage for the  $SO_2$  emissions from the coal discard. This  $SO_2$  concentration is above the current legislated maximum of 191 ppm for new power plant (IEA, 2015). In the case of the plastic sample (PL) the maximum  $SO_2$  emission occurred at 26 seconds with a concentration of 107 ppm. A reduction in the gradient of the curve indicates that less  $SO_2$  was emitted during the volatile matter combustion stage for this sample. The low  $SO_2$  emitted might be because of the regular total sulphur content of the fuel, which was reported undetected in the ultimate analysis (Figure 2). Both Figures 2 and 3 show that co-combustion of coal discard with RDF reduces  $SO_2$  emissions and changes the sample

Table I

### Proximate and ultimate analysis of the discard coal and RDF samples

Parameters	Plastic RDF (PL)	Paper blend (PB)	Discard coal (C2)
Proximate analysis (wt%, Ar)			
Fixed carbon	6.00	9.00	35.83
Volatile matter	81.67	81.15	20.17
Ash content	11.10	6.66	41.95
Moisture	1.23	3.19	2.05
Ultimate analysis (wt%, db)			
Hydrogen	9.26	8.35	2.67
Nitrogen	0.35	0.29	1.15
Total carbon	57.38	57.16	48.90
Total sulphur	UT	UT	1.34
Oxygen	20.67	24.35	1.93
CV: (MJ/kg)	31.23	22.4	16.73

ar: As received; db: dry basis; O: Oxygen by difference [100-(Ash+H+C+N+S)]; UT: untraceable

## Co-firing of high-ash discard coal and refuse-derived fuel – ash and gaseous emissions

concentration profiles. This observation agrees with the findings of other authors (Akdag, Atimtay, and Sanin., 2016, Teixeira *et al.*, 2012, Wan, 2008).

The 85% C2 plus 15% PL and 85% C2 plus 15% PB blends (Figures 2 and 3) have an emission pattern similar to that of coal discard, but at much lower concentrations. This is due to the higher coal content in this blend relative to other blends. The maximum SO<sub>2</sub> emission for 85% C2 plus 15% PL occurs at 57 seconds at a concentration of 191 ppm equal to the SO<sub>2</sub> emission limit for a new coal-fired power station in South Africa. This is a significant reduction compared to the 387-ppm produced by combustion of C2 coal alone. However, for the 85% C2 plus 15% PB blend (Figure 3), the SO<sub>2</sub> emissions exceeded the South African standard. As RDF content in the blends increased, there was a reduction in emissions with two or three peaks for some samples. For the 50% C2 plus 50% PL sample (Figure 2), three peaks were noted, with the first representing the SO<sub>2</sub> released during combustion of the PL volatile component. The second peak denotes the release of SO<sub>2</sub> during the volatile combustion of C2 and the third indicates the release of SO<sub>2</sub> from char combustion of C2. Sample 50% C2 plus 50% PB (Figure 3) displays two emission peaks at 20 seconds (110 ppm) and 49 seconds (102 ppm), which correspond to the SO<sub>2</sub> released from the combustion of the volatile matter in the blend. The alkali and alkaline-earth metal oxide contents in the two RDFs are higher than in the discard coal (Table II). These oxides might be responsible for the reduction in SO<sub>2</sub> emissions by reacting with SO<sub>2</sub> to form sulphates (Guo and Zhong, 2018).

### NO<sub>x</sub> emissions

The NO<sub>x</sub> emissions from the co-combustion of discard coal with both RDFs (PL and PB) are presented in Figure 4 and Figure 5, respectively. The plastic sample (PL, Figure 4) presents the highest peak, with two peaks displayed in its emission profile, at 17 seconds (143 ppm) and 32 seconds (119 ppm). The different volatiles associated with the fuel nitrogen and char nitrogen may be responsible for the two peaks. The dominant stage of NO<sub>x</sub> release occurred during the combustion of volatile matter for both PL and PB. For the discard coal, NO<sub>x</sub> emission peaks at 58 seconds (80 ppm), which represents the volatile combustion stage. As the reaction time increases, NO<sub>x</sub> continues to be released as the char

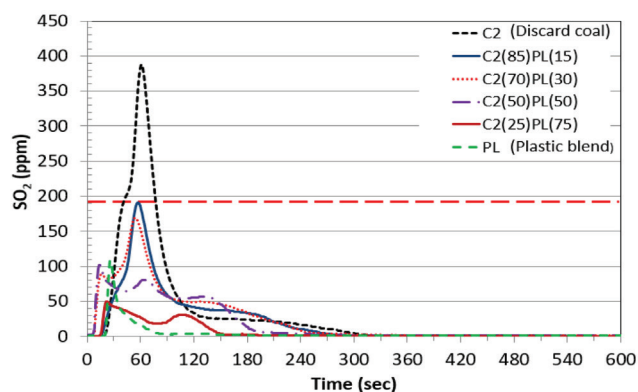


Figure 2—SO<sub>2</sub> emissions from the co-combustion of discard coal and plastic blend RDFs

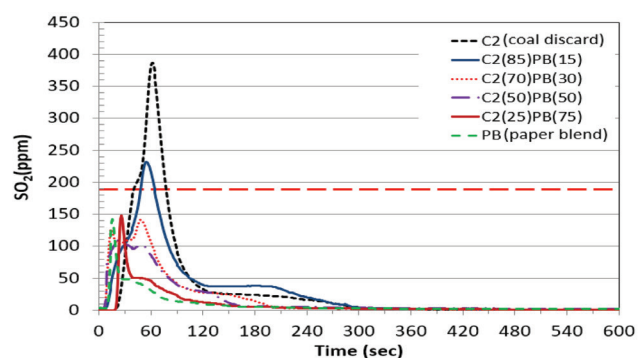


Figure 3—SO<sub>2</sub> emissions from the co-combustion of discard coal and paper blend RDF

combusts similar to the observation by Chen *et al.* (2018) during the combustion of anthracite.

With co-combustion of discard coal and PL, the 85% C2 plus 15% PL sample exhibits a similar emission profile to that of C2. NO<sub>x</sub> emissions from this sample occurred earlier at 42 seconds and a concentration of 88 ppm, which is slightly higher than the emission from 100% discard coal. The blending of PL and C2 results in a higher concentration of NO<sub>x</sub> during the volatile combustion phase and a decrease in the duration of the emissions. This is similar to the observations of Chyang, Han, Wu, Wan,

Table II

### Major elemental composition of the ash samples (wt%)

	100 % C2	100 % PB	100 % PL	70% C2 + 30% PL	25% C2 + 75% PL	70% C2 + 30% PB	25% C2 + 75% PB
Fe <sub>2</sub> O <sub>3</sub>	9.42	1.44	1.10	8.49	5.75	8.47	6.55
CaO	6.47	29.66	18.83	7.76	12.51	7.29	13.88
MgO	1.01	3.35	1.55	1.00	1.17	1.06	1.42
K <sub>2</sub> O	1.09	1.08	1.01	1.14	1.05	1.16	1.01
Na <sub>2</sub> O	1.38	13.65	8.24	1.91	4.41	2.16	4.27
SiO <sub>2</sub>	50.87	32.15	21.22	46.04	35.67	47.77	40.47
TiO <sub>2</sub>	2.51	9.04	16.71	3.98	9.18	2.83	4.82
Al <sub>2</sub> O <sub>3</sub>	34.49	73.55	45.19	34.57	43.11	34.33	41.41
SO <sub>3</sub>	3.26	8.62	4.29	5.22	9.57	4.49	11.68
Cl <sup>-</sup>	UT	0.90	2.84	0.05	0.73	UT	0.16
<b>Slagging and fouling indices</b>							
R <sub>v/a</sub>	0.22	0.43	0.37	0.24	0.28	0.24	0.31
F <sub>u</sub>	0.55	6.31	3.42	0.73	1.55	0.79	1.65

D – discard coal, PB – Paper blend RDF, PL – plastic RDF, UT – untraceable, R<sub>v/a</sub> – base-to-acid ratio, F<sub>u</sub> – fouling index



## Co-firing of high-ash discard coal and refuse-derived fuel – ash and gaseous emissions

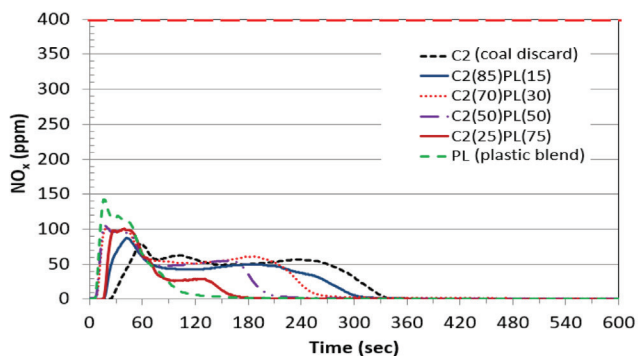


Figure 4—NO<sub>x</sub> emissions from the co-combustion of discard coal and plastic blend RDFs

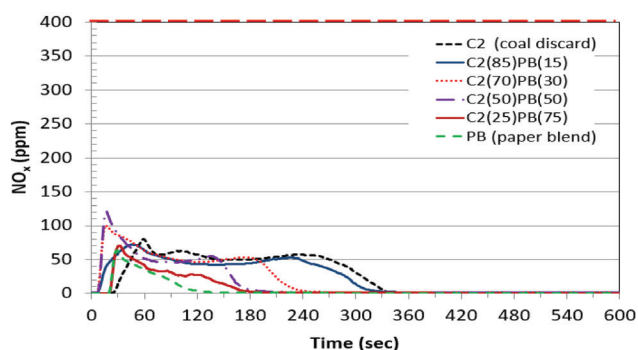


Figure 5—NO<sub>x</sub> emissions from the co-combustion of discard coal and paper blend RDF

Lee, and Chang, (2010) and Wan, Chang, Chien, Lee, and Huang, (2008) when a low coal-char component is present in a fuel. It can also be seen (Figure 4), that as the amount of coal in the blend decreases, the complete release of the NO<sub>x</sub> (char combustion) occurs earlier. The 85% C2 plus 15% PB sample displays a similar profile to that of 100% discard coal (Figure 5); however, the emission duration was shorter due to the addition of PB. The samples containing 30% and 50% PB display an emission profile with two peaks. The first peak indicates the release of NO<sub>x</sub> from the combustion of volatiles in PB. Both samples show a maximum concentration above 100% PB, indicating that there may be an interaction between the two fuels. The emission profile for the sample containing the most PB (75%) was very similar to that for 100% PB, with a maximum concentration slightly higher than 70 ppm. The NO<sub>x</sub> concentrations for most of the blends co-fired in this study are consistent with those from Wan, Chang, Chien, Lee, and Huang, (2008), who found that the emissions from co-firing of coal and RDFs remained below 100 ppm. An increase in NO<sub>x</sub> emissions was also observed by Zhang *et al.* (2018) in the co-firing of MSW with coal when the MSW content was increased above 15%. All samples conformed to the South African emission standard of 750 mg/m<sup>3</sup> (399 ppm) for NO<sub>x</sub> in new coal-fired power plants (IEA, 2015).

### CO<sub>2</sub> emissions

The emissions of CO<sub>2</sub> from the co-combustion of discard coal with RDF (Figures 6 and Figure 7) show an increasing trend as the quantity of RDF is increased. The discard coal sample shows the lowest CO<sub>2</sub> emission concentration of about 5000 ppm. CO<sub>2</sub> emissions increase as the proportion of LP in the blend increases. Samples containing 75%, 50%, and 30% LP have a two-step profile, in which the first peak is due to combustion of volatile matter.

The two peaks could relate to the two initial peaks observed in the 100% LP sample, from the combustion of its light and heavy volatile components. The second peak observed is due to the combustion of char, which gave rise to the third peak in the 100% PL sample.

The 85% C2 plus 15% PL sample displays a single-stage profile with a peak in the range of the char combustion for sample PL (the third peak) and the volatile combustion for C2, at 39 seconds and 16 000 ppm (Figure 6). The emission profile of this sample is shorter than that of 100% C2, which shows that an increase in volatile matter or PL proportion influences the CO<sub>2</sub> emission of the fuel. Volatile combustion of samples blended with 75% and 50% PL occurred at 25 seconds and 55 000 ppm, and 14 seconds and 41 000 ppm, respectively. As PL is added to the blend, the amplitude of the first peak of the emission profile increases, and that of the second peak decreases.

The CO<sub>2</sub> emission profiles the co-combustion of discard coal C2 and different paper blends are presented in Figure 7. The paper blend emitted the highest CO<sub>2</sub> concentration of all fuels, and the emissions increased as the ratio of BP in the blend increased. All paper and coal blends appeared to release CO<sub>2</sub> in a single step, indicating the combustion of volatile matter. This occurred at t<60 seconds for all the blends. The 85% C2 plus 15% PB sample emitted the lowest concentration of CO<sub>2</sub> at 25 seconds and 6000 ppm. This might be due to the large proportion of discard coal in this sample. As discussed previously, the discard coal showed very low CO<sub>2</sub> emissions, which indicates incomplete combustion of the fuel.

### Ash surface morphology

The surface morphologies of the ashes obtained from all the samples were determined using scanning electron microscopy (SEM). The micrographs of the 100% RDF samples show a

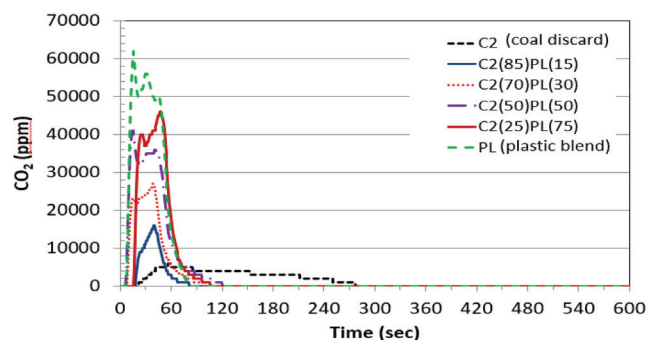


Figure 6—CO<sub>2</sub> emissions from the co-combustion of discard coal and plastic blend RDF

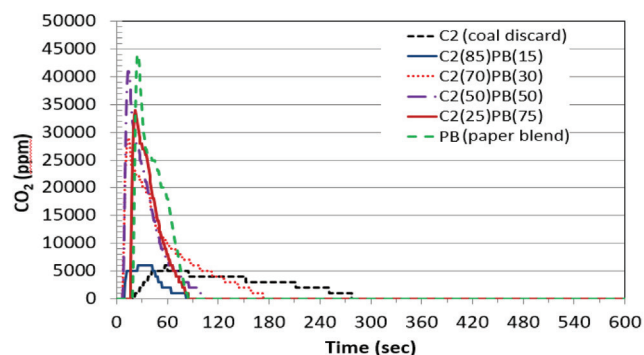


Figure 7—CO<sub>2</sub> emissions from the co-combustion of discard coal and paper blend RDF

## Co-firing of high-ash discard coal and refuse-derived fuel – ash and gaseous emissions

'shredded sponge' and 'paint chip' texture (Figures 8A and 8B). These morphologies are similar to those obtained by Taylor *et al.* (1982). The micrographs of 100% PB ash and coal blends at different proportion are seen in Figure 9. The material is heterogenous in nature and consists of very large irregular agglomerated aluminium deposits (88.92%). This could be from packaging components containing aluminium foil in the PB blend. The ash from the 100% LP (Figure 10) sample contained significantly more fine particulate matter than that from the 100% PB sample. The fine particles seen in these micrographs contain several elements, including alkali and alkaline-earth metals, which are known to form low-melting-point deposits, as well as chlorine, which causes corrosion to boiler surfaces.

The SEM image of 100% discard coal ash in Figure 9 shows that the ash contained mostly fine particles and some coarse particles consisting of Al and Si. The micrographs in Figures 9 and 10 show that as the discard coal content in the blend increases there are fewer coarse particles and more fine particles are introduced. This is consistent with the findings by Fuller *et al.* (2018). Figure 10 also shows that there are more coarse particles

sparingly distributed, in the ash from co-combustion of the coal and PL in comparison to the ash from the paper blend PB (Figure 9). The large clusters and agglomerates noted in these blends are due to the presence of low-melting-point alkaline earth metal such as Mg in the RDFs, which causes deposits within the ash, as observed by Fuller *et al.* (2018) and Wu *et al.* (2011).

### Ash elemental composition

The major elemental compositions of the ash from the PB, PL, coal discard, and their blends using XRF analysis and ion chromatography (for water-soluble chlorides) are depicted in Table II. These analyses were replicated three times to ensure reliability and an average of the results is reported.

The predominant oxides found in the 100% discard coal ash are  $\text{SiO}_2$ ,  $\text{Al}_2\text{O}_3$ ,  $\text{Fe}_2\text{O}_3$  and  $\text{CaO}$ . Silica and alumina are the most common oxide constituents found in South African coals, and are indicative of quartz ( $\text{SiO}_2$ ) and clay (Si, Al compounds) minerals. Together, these minerals generally comprise over 70% of the mineral-ash contents in South African coals (Wagner, Malumbazo, and Falcon, 2018). This result agrees with the findings of other

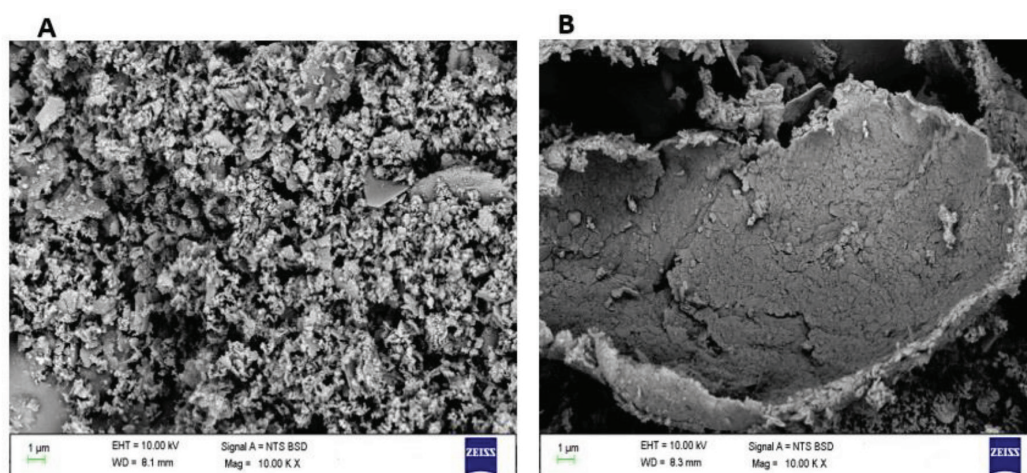


Figure 8— 'Shredded sponge' and 'paint chip' morphologies of RDF ash samples

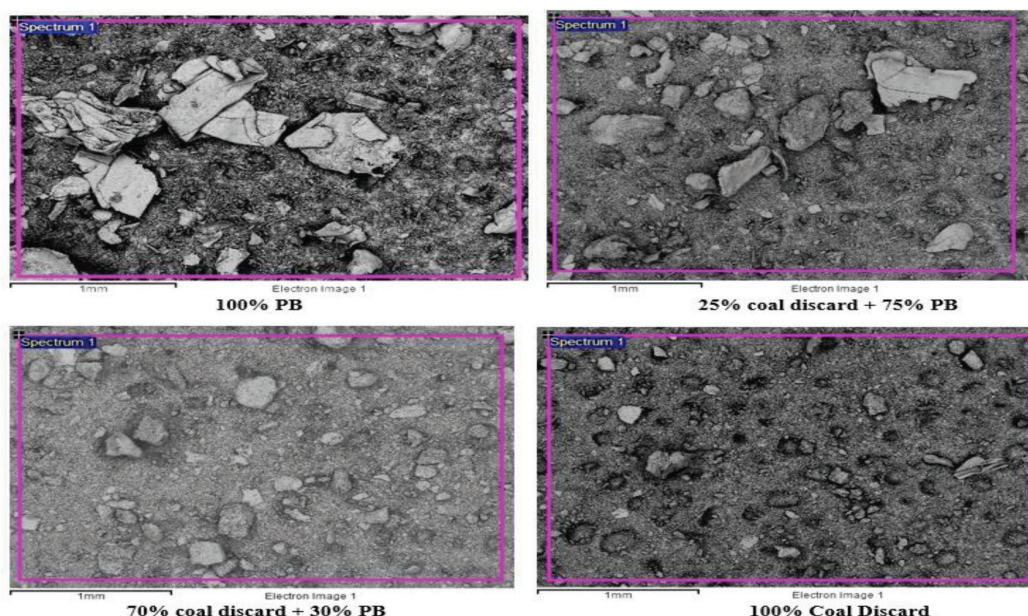


Figure 9—SEM images from the discard coal and paper blend co-combustion ash



## Co-firing of high-ash discard coal and refuse-derived fuel – ash and gaseous emissions

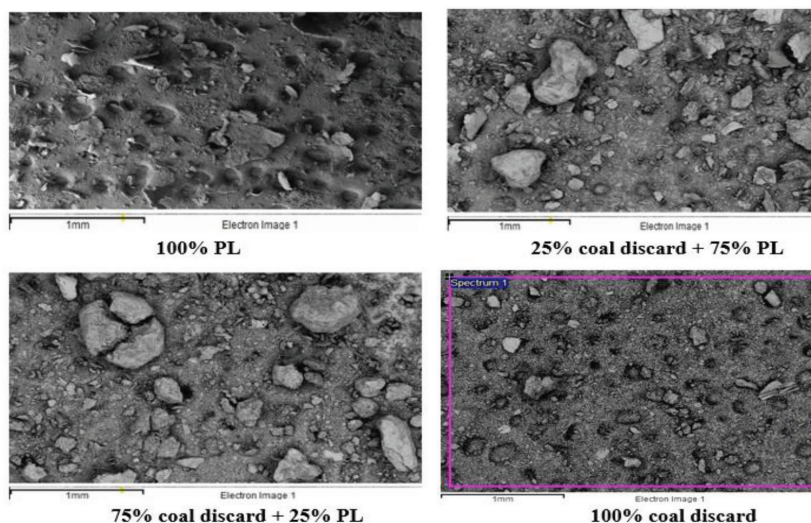


Figure 10—SEM images from the discard coal and plastic co-combustion ash

authors with regard to South African coal ash (Akinyeye *et al.*, 2016, Waanders *et al.*, 2003). The discard coal ash was found to contain 9.42%  $\text{Fe}_2\text{O}_3$  (Table II), which is higher than most of the values reported for bituminous to sub-bituminous coals in the literature. However, it can be expected that this high-ash inertinite discard coal will contain an oxide suite of minerals (CaO and MgO) and iron sulphide (pyrite, chalcopyrite *etc.*) minerals, since they are beneficiated from the organic content of the coal, leading to an increase in  $\text{Fe}_2\text{O}_3$  content.

Table II shows that the most abundant oxide in the RDF (PB and PL) ash composition was  $\text{Al}_2\text{O}_3$ , followed by  $\text{SiO}_2$ . The alkali and the alkaline-earth metal oxides are more predominant in the RDF ash than in the coal ash, indicating that these elements are present in an ionic or organic form in the RDF (Iacovidou *et al.*, 2017). Table II shows that the  $\text{SiO}_2$  content in the ash decreased with increasing RDF content in the blend, which agrees with the findings of Zhang *et al.* (2018). Table II also shows that the  $\text{Al}_2\text{O}_3$  content in the ash increased while the content of  $\text{Fe}_2\text{O}_3$  decreased as RDF is increased in the fuel blend; the same trend was observed by Wu *et al.* (2011). An increase in the CaO and  $\text{Na}_2\text{O}$  content in the ash was also noted as the proportion of RDF in the coal/RDF blend increased, with no significant change in the concentrations of MgO and  $\text{K}_2\text{O}$ . This is again consistent with the findings of Wu *et al.* (2011). The chloride content in the ash of 100% RDFs, coal discard, and their blends was determined using ion chromatography, and the results are also depicted in Table II. The plastic sample (PL) had the highest chloride concentration at 2.84%, followed by the 100% paper blend with a concentration of 0.9%. The chloride content of the coal discard sample was untraceable, which led to a decrease in the chloride content of the blend as the proportion increases. This agrees with the findings of Wan *et al.* (2008).

From the slagging and fouling indices (Table II) the 100% PB sample had the highest slagging propensity with a value of 0.43. This can be attributed to the high content of CaO and  $\text{Na}_2\text{O}$  in the fuel. The burning of this sample alone in the boiler could have a negative impact, as the alkali metal salts and alkaline-earth metals form low-viscosity deposits with low melting points. The 100% PB and PL samples showed a high propensity for fouling, with an Fu index of 6.31 and 3.42, respectively. Table II shows that the 25% discard coal plus 75% PB sample is also within the high range, due to the large quantity of PB in this sample. With an increase in the

coal proportion in the coal-RDF blends, the fouling and slagging potential is significantly reduced. Sample 25% discard coal plus 75% PL was reduced to 1.55 which is in the range for medium fouling propensity. The samples containing 30% RDF plus 70% discard coal were both close to the lower boundary for medium fouling propensity, at 0.73 and 0.79 for PL and PB, respectively.

Table II shows that the most abundant oxide in the RDF (PB and PL) ash composition was  $\text{Al}_2\text{O}_3$ , followed by  $\text{SiO}_2$ . The alkali and the alkali-earth metal oxides are more predominant in the RDF ash compared to the coal ash, indicating that these elements are present in an ionic or organic form in the RDF (Iacovidou *et al.*, 2017). Table II shows that the  $\text{SiO}_2$  content in the ash decreased with increasing RDF content in the blend, which agrees with the findings of Zhang *et al.* (2018). Table II also shows that the  $\text{Al}_2\text{O}_3$  content in the ash increased while the content of  $\text{Fe}_2\text{O}_3$  decreased as RDF is increased in the fuel blend; the same trend was observed by Wu *et al.* (2011). An increase in the CaO and  $\text{Na}_2\text{O}$  content in the ash was also noted as the proportion of RDF in the coal/RDF blend increased, with no significant change in the concentrations of MgO and  $\text{K}_2\text{O}$ . This is again consistent with the findings of Wu *et al.* (2011). The chloride content in the ash of 100% RDFs, coal discard, and their blends was determined using ion chromatography, and the results are also depicted in Table II. The plastic sample (PL) had the highest chloride concentration of 2.84%, followed by the 100% paper blend with a concentration of 0.9%. The chloride content of the coal discard sample was untraceable, which led to a decrease in the chloride content of the blend as the proportion increases. This agrees with the findings of Wan *et al.* (2008).

From the slagging and fouling indices (Table II) the 100% PB sample had the highest slagging propensity with a value of 0.43. This can be attributed to the high content of CaO and  $\text{Na}_2\text{O}$  in the fuel. The burning of this sample alone in the boiler could have a negative impact, as the alkali metal salts and alkaline-earth metals form low-viscosity deposits with low melting points. The 100% PB and PL samples showed a high propensity for fouling, with an Fu index of 6.31 and 3.42, respectively. Table II shows that the 25% discard coal plus 75% PB sample is also within the high range, due to the large quantity of PB in this sample. With an increase in the coal proportion in the coal-RDF blends, the fouling and slagging potential is significantly reduced. Sample 25% discard coal plus 75% PL was reduced to 1.55 which is in the range for medium

## Co-firing of high-ash discard coal and refuse-derived fuel – ash and gaseous emissions

fouling propensity. The samples containing 30% RDF plus 70% discard coal were both close to the lower boundary for medium fouling propensity, at 0.73 and 0.79 for PL and PB, respectively.

### Trace element concentrations

The concentrations of potentially toxic elements (PTE), such as As, Co, Cr, Cu, Mn, Ni, Sb, and V, was also investigated, and the results are reported in Table III. Concentrations of As, Co, Cr, Nd, Rb, Sr, Th, V, Y, and Zr increase as the amount of coal discard increases in the blend. As the RDF content in the blend increases the concentrations of Cu, Ga, and Zn are increased in the ash for both PL and PB. The paper blend (PB) specifically increases the concentrations of Mn, Pb, and Ni in the ash, while the plastic RDF increases the concentrations of Ba, Sn, and Sb. This agrees with the ash analyses from other RDFs and coal co-combustion studies in the literature (Taylor *et al.*, 1982, Norton, Malaby, and DeKalb, 1988).

The concentration limits of some heavy metals in ashes from Lithuania, Sweden, and Finland are depicted in Table IV (Lanzerstorfer, 2015). The ash obtained from the co-combustion of the RDF and coal used in this study conformed to the concentration limits required for most of the elements. However, the Hg concentration (Table III) in the 100% PL and blend of 25% discard coal plus 75% PL (4 ppm) was found to be above the limit. Apart from these two samples, all other ash samples could be used as a soil conditioner in forestry and agriculture in some countries, based on their stipulated heavy metal limit. The EN 450-1 (2012) standard for fly ash used in the construction industry (concrete) requires the chloride concentration in the ash to be less than or equal to 0.1%. From the results obtained in this study, both ashes produced from 100% RDFs are unsuitable for use in concrete, while the samples containing up to 70% discard coal were within the chloride limit for concrete (Table II).

### Conclusions

It was established in this study that the most favourable fuel blend that could be used for power generation is that of discard coal (25%) and PL (75%). This was based on the lowest SO<sub>2</sub> emissions attained during the volatile and char combustion of the blend. In addition to the earlier time to complete the release of the NO<sub>x</sub> (char combustion). Hence in this study, the following conclusions were made.

1. The discard coal was found to have the highest SO<sub>2</sub> and NO<sub>x</sub> emissions. With increasing RDF content in the fuel blend, a decrease in SO<sub>2</sub> and NO<sub>x</sub> emissions was observed.
2. CO<sub>2</sub> emissions increased with the addition of RDF to the blends, which could be caused by the high volatile matter content of RDF.
3. The ash obtained from the co-combustion of the discard coal and RDF showed a decrease in the alkali and alkaline-earth metal contents. This is a consequence of the increase in the proportion of coal in the blend. The water-soluble chloride content of the ash also decreased with the addition of coal to the fuel blend.

Table IV

Ash elemental concentration limits (ppm) for utilization in forestry and agriculture (Lanzerstorfer, 2015)

Trace element	Concentration (ppm)
As	30-40
Cr	100-300
Cu	400-700
Hg	1-3
Ni	70-150
Pb	150-300
Zn	700-7000

Table III

Trace elements concentrations in the co-combustion ash (ppm)

	100 % C2	100 % PB	100 % PL	70% C2 + 30% PL	25% C2 + 75% PL	70% C2 + 30% PB	25% C2 + 75% PB
As	13	3	-	11	5	10	7
Ba	713	895	2695	958	1522	912	682
Br	1	34	11	1	4	1	6
Ce	71	-	17	34	42	25	-
Co	14	19	-	53	30	31	21
Cr	254	221	164	254	230	248	244
Cu	67	353	746	135	375	79	170
Ga	52	75	79	53	65	51	62
Hg	2	1	4	2	4	2	3
Mn	437	930	188	439	340	442	620
Mo	10	12	12	11	11	11	10
Nb	39	13	37	39	39	37	28
Ni	95	111	90	84	85	86	93
Nd	200	74	124	222	215	205	181
Pb	57	104	51	56	57	62	74
Rb	50	17	13	46	36	48	39
Sb	4	79	155	22	69	49	37
Se	1	1	1	1	2	1	4
Sn	18	46	205	47	105	56	34
Sr	50	17	13	46	36	48	39
Th	47	10	10	43	34	43	35
V	192	-	-	163	34	184	127
Y	65	9	8	61	44	61	47
Zn	48	2424	3910	427	1788	182	848
Zr	476	79	145	451	331	447	322



# Co-firing of high-ash discard coal and refuse-derived fuel – ash and gaseous emissions

- The slagging and fouling indices showed that as the percentage of coal in the blend increases, the propensity of the fuel blend to slagging and fouling decreases.

## Acknowledgements

The authors gratefully acknowledge the financial support of National Research Foundation of South Africa's SARChI Clean Coal Technology Grant (Grant Number: 86421). Opinions, findings, and conclusions expressed are those of the authors and NRF accepts no liability whatsoever in this regard. In addition, the authors express their appreciation to Interwaste, South Africa for providing the refuse-derived waste used in this study.

## References

- AKINYEYE, R., OMONIYI, P., LESLIE, P., and OLORUNFEMI, O. 2016. Comparative chemical and trace element composition of coal samples from Nigeria and South Africa. *American Journal of Innovative Research & Applied Sciences*. pp. 391–404.
- AKDAG, A., ATIMTAY, A., and SANIN, F. 2016. Comparison of fuel value and combustion characteristics of two different RDF samples. *Waste Management*, vol. 47. pp. 217–224.
- BREW, M. What's on the horizon for refuse-derived fuel as Brexit looms and production evolves. <https://www.recyclingwasteworld.co.uk/in-depth-article/as-brexit-looms-and-production-evolves-whats-on-the-horizon-for-refuse-derived-fuel/172555/> (accessed 25 March 2022).
- CHEN, X., XIE, J., MEI, S., and HE, F. NO<sub>x</sub> and SO<sub>2</sub> 2018. emissions during co-combustion of rdf and anthracite in the environment of precalciner. *Energies* vol. 11. <https://doi.org/10.3390/en11020337>
- CHENG, G. and ZHANG, C. 2018. Desulfurization and denitrification technologies of coal-fired flue gas. *Polish Journal of Environmental Studies*, vol. 27, no. 2. pp. 481–89.
- CHYANG, C.S., HAN, Y.L., WU, L.W., WAN, H.P., LEE, H.T., and CHANG, Y.H. 2010. An investigation on pollutant emissions from co-firing of RDF and coal. *Waste Management*, vol. 30. pp. 1334–1340.
- DEA. 2018. South Africa State of Waste Report. Department of Environmental Affairs, Pretoria.
- DEA. 2012. Municipal Solid Waste Tariff Strategy. Department of Environmental Affairs, Pretoria.
- ESKOM, n.d. ESKOM HOLDINGS SOC LTD - LETHABO POWER STATION. [https://web.archive.org/web/20090713043507/http://www.eskom.co.za/live/content.php?Item\\_ID=179](https://web.archive.org/web/20090713043507/http://www.eskom.co.za/live/content.php?Item_ID=179) [accessed 25 March 2022].
- FFF. 2017. Fossil Fuel Foundation of Africa. Submission to the Department of Energy RE. South African Integrated Resource Plan 2016 (unpublished).
- FULLER, A., MAIER, J., KARAMPINIS, E., KALIVODOVA, J., GRAMMELIS, P., and KAKARAS, E., 2018. Fly ash formation and characteristics from (co-)combustion of an herbaceous biomass and a Greek lignite (low-rank coal) in a pulverized fuel pilot-scale test facility. *Energies*, vol. 11, no. 6. <https://doi.org/10.3390/en11061581>
- GUO, F. and ZHONG, Z. 2018. Co-combustion of anthracite coal and wood pellets: Thermodynamic analysis, combustion efficiency, pollutant emissions and ash slagging. *Environmental Pollution*, vol. 239. pp. 21–9. <https://doi.org/10.1016/j.envpol.2018.04.004>
- IACOVIDOU, E., HAHLADAKIS, J., DEANS, I., VELIS, C., and PURNELL, P. 2018. Technical properties of biomass and solid recovered fuel (SRF) co-fired with coal: Impact on multi-dimensional resource recovery value. *Waste Management*, vol. 73. pp. 535–45. <https://doi.org/10.1016/j.wasman.2017.07.001>
- IEA. 2015. Emission Standards: South Africa, London.
- JAMES, A.K., THRING, R.W., HELLE, S., and GHUMAN, H.S. 2012. Ash management review-applications of biomass bottom ash. *Energies*, vol. 5. pp. 3856–7383. <https://doi.org/10.3390/en5103856>
- LANZERSTORFER, C. 2015. Chemical composition and physical properties of filter fly ashes from eight grate-fired biomass combustion plants. *Journal of Environmental Science (China)*, vol. 30. pp. 191–197. <https://doi.org/10.1016/j.jes.2014.08.021>
- MAKWARELA, M.O., BADA, S.O., and FALCON R.M.S. 2017. Co-firing combustion characteristics of different ages of *Bambusa balcooa* relative to a high ash coal. *Renewable Energy*, vol. 105. pp. 656–664.
- MALAT'ÁK, J., VELEBIL, J., and BRADNA, J. 2018. Specialty types of waste paper as an energetic commodity. *Agron Res*, vol. 16. pp. 534–42. <https://doi.org/10.15159/AR.18.045>
- MILLER, B. 2011. Clean Coal Engineering Technology. 2nd edn.
- NDOU, N.R., BADA, S.O., FALCON, R.M.S., and WEIERSBYE, I.M. 2020. Co-combustion of *Searsia lancea* and *Tamarix usneoides* with high ash coal. *Fuel*, vol. 267. 117282.
- NORTON, G.A., MALABY, K.L., and DEKALB, E.L. 1988. Chemical characterization of ash produced during combustion of refuse-derived fuel with coal. *Environmental Science and Technology*, vol. 22. pp. 1279–83. <https://doi.org/10.1021/es00176a005>
- RAUTENBACH, R. STRYDOM, C.A. BUNT, J.R. MATJIE, R.H., CAMPBELL, Q.P., and VAN ALPHEN, C. 2019. Mineralogical, chemical, and petrographic properties of selected South African power stations' feed coals and their corresponding density separated fractions using float-sink and reflux classification methods. *International Journal of Coal Preparation and Utilization*, vol. 39, no. 8. pp. 421–446.
- SETSEPU, R.L., ABDUSALAM, J., and BADA, S.O. 2021. Effects of *Searsia lancea* hydrochar inclusion on the mechanical properties of hydrochar/discard coal pellets. *Journal of the Southern African Institute of Mining and Metallurgy* 2021, vol. 121. pp. 617–621.
- TAYLOR, D.R., TOMPKINS, M.A., KIRTON, S.E., MAUNEY, T., NATUSCH, D.F.S., and HOPKE P.K. 1982. Analysis of fly ash produced from combustion of refuse-derived fuel and coal mixtures. *Environmental Science and Technology*, vol. 16. pp. 148–54. <https://doi.org/10.1021/es00097a006>
- TEIXEIRA, P., LOPES, H., GULYURTLU, I., LAPA, N., and ABELHA, P. 2012. Evaluation of slagging and fouling tendency during biomass co-firing with coal in a fluidized bed. *Biomass and Bioenergy*, vol. 39. pp. 192–203. <https://doi.org/10.1016/j.biombioe.2012.01.010>
- VEKEMANS, O. and CHAOUKI, J. 2016. Municipal solid waste co-firing in coal power plants: Combustion Performance. *Developments in Combustion Technology*. pp. 118–42. <https://doi.org/http://dx.doi.org/10.5772/63940>
- WAANDERS, F., VINKEN, E., MANS, A., and MULABA-BAFUBIANDI, A. 2003. Iron minerals in coal, weathered coal and coal ash – SEM and Mössbauer results. *Hyperfine Interact*, vol. pp. 35–7. <https://doi.org/10.1023/B:HYPE.0000003760.89706.f6>
- WAGNER, N., MALUMBAZO, and FALCON, R.M.S. 2018. Southern African Coal and Carbon Petrographic Atlas: Definitions and Applications of Organic Petrology. Penguin.
- WAN, H.P., CHANG, Y.H., CHIEN, W.C., LEE, H.T., and HUANG, C.C. 2008. Emissions during co-firing of RDF-5 with bituminous coal paper sludge and waste tires in a commercial circulating fluidized bed co-generation boiler. *Fuel*, vol. 87. pp. 761–767. <https://doi.org/10.1016/j.fuel.2007.06.004>
- WORLD BANK. 2019. Solid Waste Management. <http://www.worldbank.org/en/topic/urbandevelopment/brief/solid-waste-management> [accessed 23 October 2021].
- WU, H., GLARBORG, P., FRANSEN, F.J., DAM-JOHANSEN, K., JENSEN, P.A., and SANDER, B. 2011. Co-combustion of pulverized coal and solid recovered fuel in an entrained flow reactor - General combustion and ash behaviour. *Fuel*, vol. 90. pp. 1980–91. <https://doi.org/10.1016/j.fuel.2011.01.037>
- ZHANG, S., LIN, X., CHEN, Z., LI, X., JIANG, X., and YAN, J. 2018. Influence on gaseous pollutants emissions and fly ash characteristics from co-combustion of municipal solid waste and coal by a drop tube furnace. *Waste Management*, vol. 81. pp. 33–40. <https://doi.org/10.1016/j.wasman.2018.09.048>. ◆